MULTI-OBJECTIVE DESIGN STUDY OF A FLAPPING WING GENERATOR

Eriko Shimizu
Integrated Fluid Informatics Laboratory, Institute of Fluid Science, Tohoku University

Keywords: *Power generation, Flutter, Flapping wing, Multi-objective optimization, Aeroelasticity*

Abstract

"Flapping Wing Power Generator" extracts wind energy from the flutter phenomenon. The system is governed by six non-dimensional design parameters. Present study carried out a multi-objective design for efficiency and power, and revealed the behavior of the system in detail. To obtain a wide variety of Pareto solutions efficiently, Adaptive Neighboring Search (ANS), one of Evolutionary Algorithms, has been extended to handle multiple objectives in the present study. Tradeoff between efficiency and power was obtained, and the behavior of the system was discussed.

1 Introduction

As is well known, "flutter" is a destructive aeroelastic phenomenon that must be avoided in aeronautical/industrial structures such as aircrafts and suspension bridges. The present study, however, deals with a power generation system which extracts wind energy from flutter phenomenon by utilizing it.

The idea of extracting wind energy from flutter phenomenon is not new. "Flutter Engine" by Duncan [1] might be the first machine, although it was originally built for explaining the flutter phenomenon, and not for the wind power generator.

Mckinney and DeLaurier [2] proposed the "Wingmill" which utilized a harmonically oscillating wing to extract wind energy. The whole (rectangular) wing oscillates in vertical translation and pitching with prescribed phasing between the two motions. The concept of Mckinney and DeLaurier's Wingmill has no elastic support, and the heaving and pitching motions are mechanically coupled. They conducted wind tunnel experiments with a working model and obtained power generation efficiency which was comparable to a rotary windmill.

Jones *et al*. [3] have also presented the results of their design study of a similar Wingmill. They employed a panel code as the aerodynamic evaluation tool, and predicted higher efficiency than that obtained by Mckinney and DeLaurier.

Recently, Isogai *et al*. [4] proposed a new system. In their system, the wing is supported elastically in the heaving oscillation while the pitching oscillation of the whole wing is mechanically driven by an electric motor with a prescribed frequency and pitch amplitude. This system is governed by six non-dimensional parameters. In Ref. [4], these design parameters were optimized to maximize efficiency by using "Complex Method" proposed by Box [5]. The resultant system achieves 49% power efficiency and 6.99kW work (the wing semi-chord is 0.5[m], span is 10[m], assumed wind speed is 15[m/s]).

This paper considers multi-objective optimization of Isogai's "Flapping Wing Power Generator" to maximize efficiency and power. To obtain a wide variety of Pareto solutions efficiently, one of Evolutionary Algorithms, Adaptive Neighboring Search (ANS) proposed by Takahashi [6] has been extended for multiple objectives in the present study. Multi-objective optimization reveals design tradeoff of the system.

2 The Device Concept

In the flapping generator, the motion of the wing consists of heaving and pitching (Fig.1). Pitching is given by an electric motor at prescribed frequency and amplitude. Heaving induced from pitching motion is supported elastically.

The concept of this system is as follows: the lift induced from the pitching oscillation generates the heaving oscillation. The power extracted from the system is given by the work from the lift causing the wing heaving. The power needed for pitching motion was only less than 1% of the overall power [4].

The wing used in the present study has NACA 0012 section, semi-chord length of 0.5[m], span of 1[m]. The amplitude of the forced pitching motion given by the motor is 50[deg]. Free stream velocity is 15[m/s].

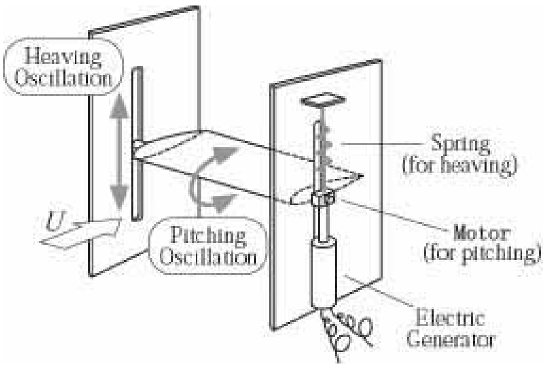

Fig.1 The concept of flutter wing generator

3 Method of Analysis

Based on the potential theory, the governing equation of the motion of this system can be derived as follows:

$$M_h d^2H/dT^2 + \omega_h^2 M_h(1+ig)H = L + M_w(X_{cg} - A)d^2\alpha/dT^2 \qquad (1)$$

where T is time, H is the vertical displacement of the wing (positive up), α is the angular displacement (positive nose-up) of the forced pitching oscillation, M_h is the total mass relating to the heaving oscillation (including wing, electric motor, etc.), ω_h is the natural circular frequency of the heaving oscillation, g is the artificial structural damping coefficient added to the system to maintain harmonic oscillation with constant amplitude, A is the location of the axis of pitch, X_{cg} is the location of the center of mass of the wing, M_w is the mass of the wing, and L is the lift (positive up). Readers may refer to Ref. 4 for details. To solve equation (1), analytical expressions of two-dimensional unsteady aerodynamic forces given in Ref. [7] are employed. The designer must give the wing semi-chord length b, span l, free stream velocity U and the forced pitching amplitude α_0.

From a nondimensional variation of equation (1), we can state that the aerodynamic response of this system is governed by six design parameters: a (dimensionless location of the axis of pitch), x_{cg} (dimensionless location of the center mass of the wing), k (reduced frequency), g (artificial structural damping coefficient), μ (mass ratio), ω_h/ω (rate of frequency: ω_h is the natural circular frequency of the heaving oscillation, while ω is the circular frequency of the forced pitching oscillation).

To simplify the design, the location of the axis of pitch is fixed at the center mass of the wing. With this assumption, the second term of the right hand side of equation (1) can be deleted. So design parameters are reduced to five.

Assuming the wing motion is simple harmonic oscillation, we can obtain an analytical solution of equation (1) from the five design parameters. Mean work provided by aerodynamic force *i.e.* the wind energy extracted from the flapping generator system is given as equation (2).

$$W = \frac{1}{T^*}\oint\left(L\dot{H} + M_\alpha \dot{\alpha}\right)dt \qquad (2)$$

And the efficiency is given by

$$\eta_p = W/\left(1/2\,\rho U^3(2H_s)l(16/27)\right) \qquad (3)$$

In equation (2) T^* is oscillation frequency, M_α is pitching moment induced from aerodynamic. In equation (3) 16/27 shows Betz coefficient [8]. H_s shows the leading-edge or trailing-edge amplitude and whichever is larger is used.

4 Method of Optimization

In this study, the system is optimized by ANS-M. ANS-M is based on ANS (Adapted Neighboring Search) and extended for multi-objective optimization in the present study.

ANS is an Evolutionary Algorithm, which uses real-coded representation and crossover-like mutation based on the normal distribution for generating next searching points. This Gaussian distribution is formed based on the relative position between an individual and its neighbors. This algorithm produces emergent of clusters of individuals within the population as a result of evolution. Those clusters search design space independently and find multiple optima efficiently. ANS proceeds as follows.

1. Pick up a core individual from the population.
2. Define a neighborhood and select individuals in a neighborhood as "neighbors".
3. Generate children from the core and neighbors.
4. Calculate their fitness values.
5. Select the best individual and put it back into the population instead of the core.

Steps 1-3 are called XLM (UNDX-m like mutation). The detailed procedure is shown in the Appendix.

In ANS-M, Steps 1-3 are the same as those of ANS. But Steps 4-5 are modified. Changes are as follows.

4'. Calculate their rank using Pareto ranking method.

5'. Select superior individuals having good rank in the several number of the objective functions and put them back to the population instead of the core and neighbors.

These modifications enable ANS-M to adapt to multi-objective problems and to obtain a wide variety of Pareto solutions.

ANS-M is tested on several test functions, which include constrained problems, and showed good results.

5 Objective Functions and Design Parameters

In the current study, objective functions are efficiency and power. These are shown as equations (2) and (3).

Design parameters are as follow: a (location of the axis of pitch), k (reduced frequency), g (artificial structural damping coefficient), μ (mass ratio), ω_h/ω (rate of frequency: ω_h is the natural circular frequency of heaving oscillation, while ω is the circular frequency of the forced pitching oscillation). They are bounded as follows.

$$-1.0 < a < 1.0$$
$$k < 0.3$$
$$0.0 \le g \le 1.0$$
$$5.0 < \mu < 200.0$$
$$0.5 < \omega_h/\omega < 1.5$$

The system is also constrained as follows.

$$0.5 < H_0/b < 2.0$$
$$100 < \phi\,[\text{deg}] < 150$$
$$1.0 < W\,[\text{kW}]$$
$$W_2 < 0.0$$

where H_0 is the amplitude of the heaving oscillation, ϕ is the phase delay angle of the heaving oscillation with respect to the forced pitching oscillation, and W is the total power generated, which is the sum of W_1 and W_2, where W_1 is the work done by lift and W_2 is the work done by the pitching moment. These constraints are imposed so that the dynamic stall phenomenon gives favorable effects on the power generation. According to numerical simulations using a Navier-Stokes code [9], the dynamic stall phenomenon reduces both the efficiency and the power considerably if these constraints are not imposed. By applying these constraints to k, ϕ and W_2, it is guaranteed that the dynamic stall phenomenon increases both the efficiency and the power, beyond those predicted by the potential code.

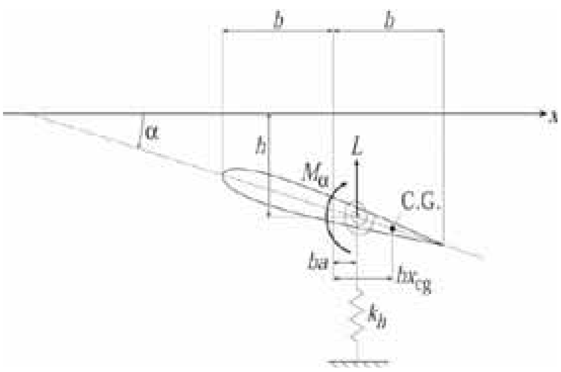

Fig. 2 The model of two dimensional flapping wing

6 Results

After 4000 generations, we obtain 321 non-dominated solutions. Figures 3-8 show non-dominated solutions. Power is shown per unit span length. In figure 3, vertical axis indicates power and horizontal axis indicates efficiency. We can see tradeoff between power and efficiency. When the efficiency becomes over 0.45, power sharply decreases. Table 1 shows optimal solutions, one has the largest efficiency (ANS(I)), the other has the largest power (ANS(II)).

In figure 4, vertical axis indicates rate of frequency and horizontal axis indicates location of axis of pitch. This figure shows that the location of axis of pitch tends to be around 0.4 and rate of frequency tends to be around 0.9.

In figure 5, vertical axis indicates the mass ratio and horizontal axis indicates the artificial structural damping coefficient. According to figure 5, we can see a correlation between artificial structural damping coefficient and mass ratio.

In figure 6, vertical axis indicates phase advance angle, horizontal axis indicates dimensionless heaving amplitude. This figure shows that phase delay angle becomes more than 100[deg] around where dimensionless heaving amplitude is around 1.

In figures 7 and 8, vertical axis indicates efficiency and power, respectively, and horizontal axis indicates reduced frequency. We can see a linear relation between reduced frequency and efficiency and between reduced frequency and power. As reduced frequency increases, power decreases and efficiency increases. But the linear relation is broken around k (reduced frequency) = 0.3 in figure 8.

To clarify the effect of reduced frequency to the system, the system was optimized with the other design parameters fixed (a = 0.39, g = 0.59, μ = 20.8, $\omega_h/\omega = 0.88$). The result is shown in figure 9. This graph shows that as reduced frequency increases, efficiency also increases but power decreases. Since, by definition, the efficiency is divided by the amplitude of heaving oscillation which increases as the reduced frequency increase, efficiency increases as the reduced frequency increases.

Furthermore, to see the relation between mass ratio and artificial structural damping coefficient, the system was optimized with the other design parameters fixed (a = 0.39, k = 0.3, $\omega_h/\omega = 0.88$). Results are shown in figures 10-12. In figure 10, vertical axis indicates mass ratio and horizontal axis shows artificial structural damping coefficient. This graph shows that the relation between mass ratio and artificial structural damping coefficient has a peak at g = 0.99. In figure 11 and 12, vertical axis indicates power and efficiency. Horizontal axis shows each artificial structural damping coefficient and mass ratio. Figure 12 shows that mass ratio increases sharply from 8 to 9 and then it increases moderately.

Future work is to clarify the relation between mass ratio and artificial structural damping coefficient. The peak may be induced from the resonance of the system, but more research is needed.

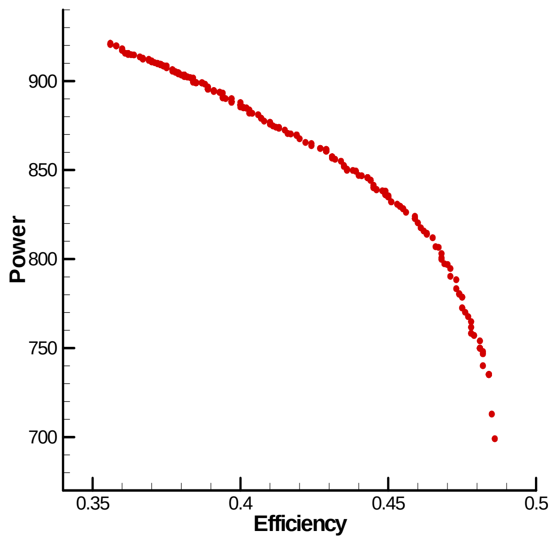

Fig. 3 Power of non-dominated solutions plotted to efficiency

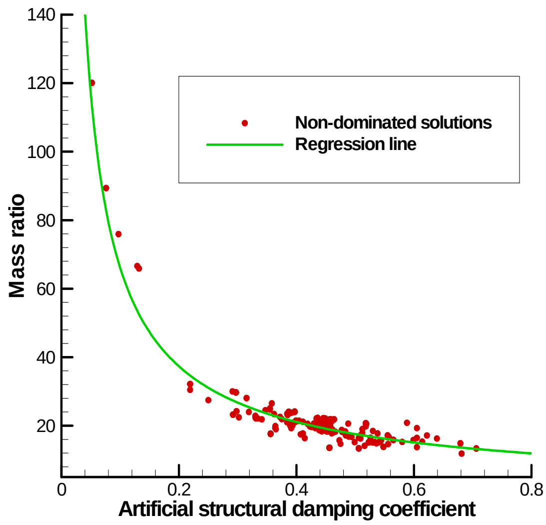

Fig. 5 Mass ratio of non-dominated solutions plotted to artificial structural damping coefficient

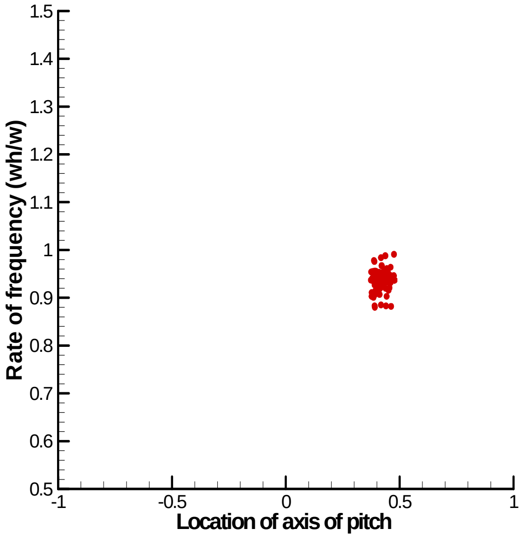

Fig.4 Rate of frequency of non-dominated solutions plotted to location of axis

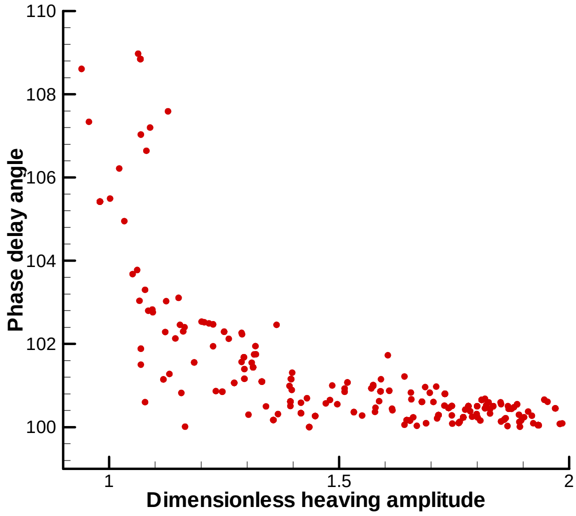

Fig. 6 Phase delay angle of non-dominated solutions plotted to dimensionless heaving amplitude

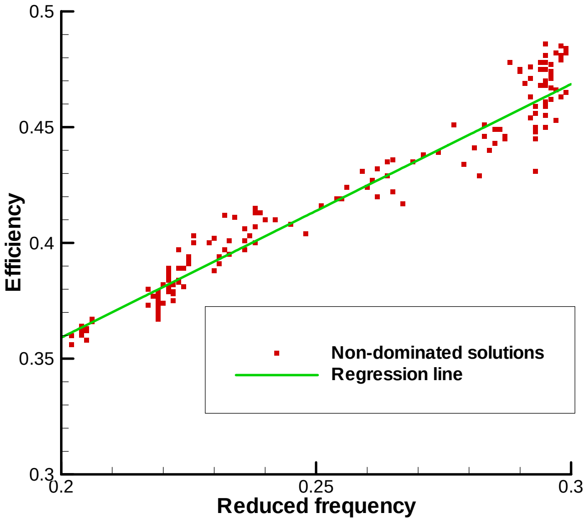

Fig. 7 Efficiency of non-dominated solutions plotted to reduced frequency

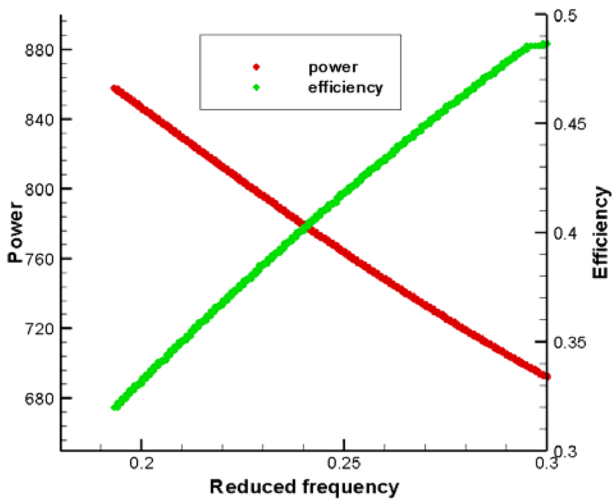

Fig. 9 Reduced frequency of non-dominated solutions plotted to power and efficiency. Other parameters are fixed.

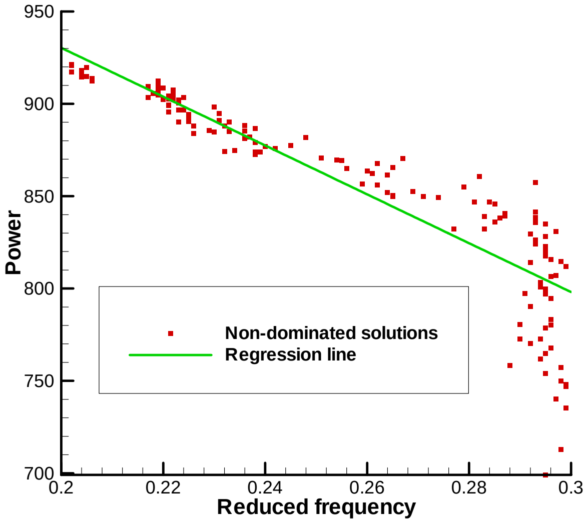

Fig. 8 Power of non-dominated solutions plotted to reduced frequency

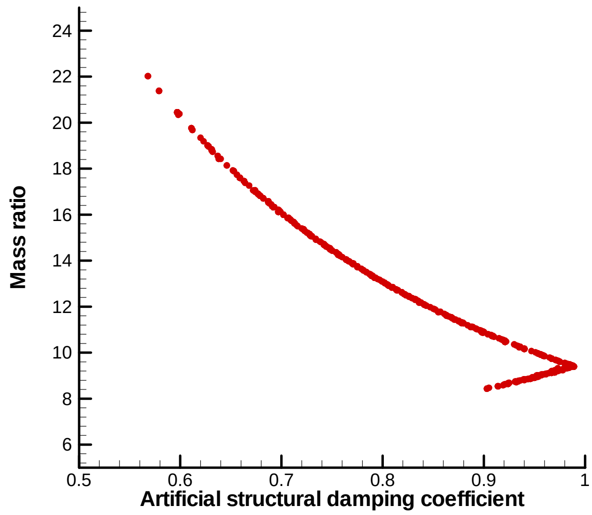

Fig. 10 Mass ratio of non-dominated solutions plotted to artificial structural damping coefficient. Other parameters are fixed.

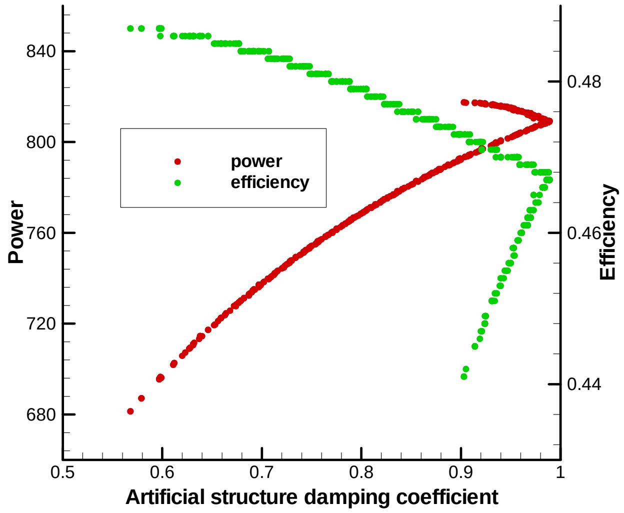

Fig. 11 Artificial structural damping coefficient of non-dominated solutions plotted to power and efficiency. Other parameters are fixed.

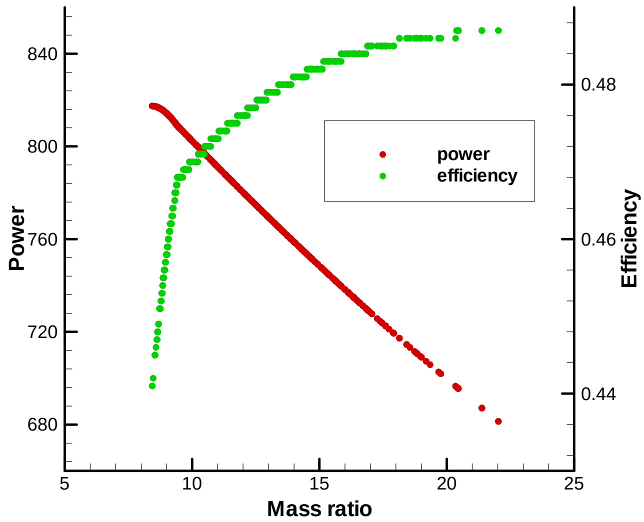

Fig. 12 Mass ratio of non-dominated solutions plotted to power and efficiency. Other parameters are fixed.

7 Conclusions

Present study has been conducted multi-objective optimization of a power generation system, which extracts wind energy from the aeroelastic response of an elastically supported rectangular wing. The result revealed tradeoff between efficiency and power from non-dominated solutions (Fig. 3). Furthermore design parameters are observed to have specific relations (Fig. 4, 5). Figures 7 and 8 suggest the reduced frequency is the dominant parameter of the system. To confirm this observation, the system is optimized by fixing the design parameters except for the reduce frequency. The result represents the linear tradeoff between efficiency and power.

Multi-objective optimization helps designers to understand the system behavior and thus to design a better system.

	a	k	g	μ	ω_h/ω	H_0/b	ϕ	Efficiency[%]	Power[kW]
Complex	0.41	0.30	0.47	23.8	0.90	0.94	110	49	6.99
ANS(I)	0.39	0.30	0.59	20.8	0.94	0.94	109	49	6.99
ANS(II)	0.40	0.20	0.43	22.1	0.95	1.99	100	36	9.21

Table 1 Design parameters and performances of non-dominated solutions. Power is shown for span length of 10 [m].

References

[1] Duncan, J. W. The fundamentals of flutter, R&M No. 2417, pp 1-36, Nov. 1948.

[2] McKinney, W. and DeLaurier, J., The wingmill: An oscillating-wing windmill. *Journal of Energy*, Vol. 5, No. 2, pp 109-115, March-April, 1981.

[3] Jones, K., Platzer, M. F. and Davis, S., Oscillating-wing power generator, FEDSM99-7050, Proceedings of ASME/JSME FEDSM799, *1999 ASME/JSME Fluid Engineering Division Summer Meeting*, San Francisco, California, July 18-23, 1999.

[4] Isogai, K., Yamasaki, M., Matsubara, M., and Asaoka, T., Design study of Elastically Supported Flapping Wing Power generator, *International forum on Aeroelasticity and Structural Dynamics 2003* (CD-ROM), Amsterdam, June 4-6, 2003.

[5] Box, M. J., A new method of constrained optimization and a comparison with other methods, *Computer Journal*, Vol. 8, pp 42-52, 1965.

[6] Takahashi, O., Kobayashi, S., An adaptive Neighboring Search using Crossover-like Mutation for Multimodal Function Optimization, *IEEE International Conference on system, Man and Cybernetics*, pp 261-267, 2001.

[7] Theodorsen, T., General theory of aerodynamic instability and mechanism of flutter, NACA Report 496, 1935.

[8] Johnson, G. L., *Wind energy systems*, Prentice Hall Inc., Englewood Cliffs, NJ, 1985

[9] Isogai, K., Shinmoto, Y. and Watanabe, Y., Effect of dynamic stall on propulsive efficiency and thrust of flapping airfoil, *AIAA Journal*, Vol. 37, No. 10, pp 1145-1151, Oct. 1999.

APENDIX

UNDEX-m like mutation procedure

1. Select one individual $\boldsymbol{x}^0$ as a core randomly from the population
2. Select m individuals $\boldsymbol{x}^1,\ldots,\ \boldsymbol{x}^m$ randomly from neighbors.
3. Let the difference vector of the individuals $\boldsymbol{x}^1,\ldots,\boldsymbol{x}^m$ be $\boldsymbol{d}^i = (\boldsymbol{x}^i - \boldsymbol{x}^0)/2$
4. Select one more individual $\boldsymbol{x}^{m+1}$ randomly from neighbors
5. Let D be the length of component of $\boldsymbol{d}^{m+1} = \boldsymbol{x}^{m+1} - \boldsymbol{x}^0$ orthogonal to $\boldsymbol{d}^1,\ldots,\boldsymbol{d}^m$
6. Let $\boldsymbol{e}^1,\ldots,\boldsymbol{e}^{n-m}$ be a orthonormal bases of the subspace orthogonal to the subspace spanned by $\boldsymbol{d}^1,\ldots,\boldsymbol{d}^m$
7. Generate offspring $\boldsymbol{x}^c$ by the following equation:

$$x^c = p + \sum_{k=1}^{m} \omega_k d^k + \sum_{k=1}^{n-m} \upsilon_k D e^k \qquad \text{(A-1)}$$

where ω_k and υ_k are Gaussian random numbers given by $N(0,\sigma_\xi)$, $N(0,\sigma_\eta)$, respectively, and σ_ξ and σ_η are shown as follows.

$$\sigma_\xi = \frac{1}{\sqrt{m}}, \sigma_\eta = \frac{0.35}{2\sqrt{n-m}} \qquad \text{(A-2)}$$